Vortex Phase Diagram of $Bi_2Sr_2CaCu_2O_{8-y}$ near the Superconducting Transition

Y. M. Wan, S. E. Hebboul, and J. C. Garland
Department of Physics, Ohio State University, Columbus, Ohio 43210
(Received 2 February 1994)

Six-terminal measurements of the resistive transition of $Bi_2Sr_2CaCu_2O_{8-y}$ crystals in a weak external magnetic field $H \parallel c$ *axis* are analyzed to deduce the magnetic H-T phase diagram near the superconducting transition. We find evidence for two magnetic field boundaries, namely, a depinning field $H_p(T)$, and a 3D-2D crossover field $H_m(T) \geq H_p(T)$, each of which intersects the $H = 0$ axis at a temperature above the zero-field a-b plane transition temperature. We interpret the crossover field $H_m(T)$ as marking the boundary between 3D vortex lines and interacting 2D vortices.

PACS numbers: 74.40.+k, 74.60.Ge, 74.72.Hs

The magnetic properties of the highly anisotropic $Bi_2Sr_2CaCu_2O_{8-y}$ (Bi:2212) layered superconductor are characterized by unusual quasi-two-dimensional vortex states and have thus become the subject of extensive investigations [1–5]. Recently, several key mixed-state measurements in Bi:2212 crystals have been interpreted as evidence for two-dimensional (2D) vortices (throughout a wide portion of the H-T phase diagram) [1], flux creep crossover and relaxation over surface barriers [2], low-temperature vortex glass behavior [3], vortex fluctuations [4], and an irreversibility line with a dimensionality crossover [5]. Aside from Ref. [4], a common feature of these studies is their effort to probe the global nature of the phase diagram, testing issues involving entanglement [6], flux creep [7], vortex glass behavior [8], and melting [6, 9], but without addressing specifically the convergence of the possible vortex phase boundaries near the superconducting transition. In the work reported here, we address this issue by exploring the structure of the weak-field phase boundaries just below the mean-field transition temperature, where thermal excitations tend to disrupt the alignment of 2D "pancake" vortices [10].

It has been observed [11] that the zero-field resistive transition of Bi:2212 crystals is characterized by separate a-b plane and c axis transition temperatures T_c^{ab} and T_c^c, with $T_c^c - T_c^{ab} \sim 2$ K. Consistent with this observation, Brawner *et al.* [4] have recently reported that both the a-b plane critical current J_c and the penetration field H_p fall to zero approximately 2–3 K below T_c. Similar results have also been obtained by Schilling *et al.* [5], who observed an abrupt disappearance of the irreversibility line several degrees below T_c. Although these measurements have effectively brought the accessible range of the H-T phase diagram closer to T_c, and renewed speculations about possible reentrant phases [4, 8], the relevant phase boundaries near T_c remain unresolved.

In this work, we have performed six-terminal transport measurements of Bi:2212 crystals in small external magnetic fields ($H < 50$ Oe) applied parallel to the c axis. Using a "dc flux-transformer" electrode configuration [12], which essentially probes the interlayer coupling of a-b plane 2D vortices, we obtain the H-T phase diagram near T_c by analyzing the behavior of the secondary voltage $V_s(T, H)$ as a function of temperature and field. We find no evidence for a reentrant superconducting phase above the a-b plane transition temperature T_c^{ab}. Instead, our results suggest that in the region just below T_c^c, the H-T phase diagram of Bi:2212 is characterized by two boundaries, a flux depinning field $H_p(T)$ and a 3D-2D crossover field $H_m(T)$, each of which intersects the $H = 0$ line at a critical point T_m, with $T_m - T_c^{ab} \sim 0.2 \pm 0.1$ K. In the small H-T region defined by $T_c^{ab} < T < T_m$ and $0 < H < H_p$, magnetic flux is expelled from the sample even though the CuO bilayers are resistive.

Our measurements were performed on three Bi:2212 single crystals which were prepared by a standard solid state melt process [11], and which displayed superconducting transitions in the range 85–88 K. Typical sizes of the cleaved crystals were 1.0 mm × 0.5 mm × 0.02 mm, with the c axis oriented along the smallest dimension. Representative a-b plane and c axis resistivities at 100 K were $\rho_{ab} \approx 4.0 \times 10^{-4}\ \Omega$ cm and $\rho_c \approx 1.5\ \Omega$ cm, yielding anisotropy ratios of 10^3–10^4. Up to six electrodes were fabricated by bonding Au wires or foils with Ag paste to each sample, producing contact resistances of 5 Ω or less. The samples were mounted inside a variable-temperature cryostat immersed in a ^{4}He bath, and the temperature was monitored with a carbon-glass thermometer over the range 4–300 K. Temperatures were regulated between 4 and 100 K with an absolute accuracy of 0.1 K and a stability of 20 mK or less. Flux-transformer voltages and a-b plane current-voltage (IV) characteristics were recorded using a four-terminal technique in which square wave currents (16.9 Hz, 1 μA–6 mA) were applied to the sample and the voltage detected with a lock-in amplifier with 1 nV resolution.

To investigate interlayer vortex correlations in external fields $H \parallel c$ *axis*, small currents I_p (< 0.5 mA, typically) were applied parallel to the primary CuO bilayers (top face), with the voltage drop $V_s(T, H)$ in the secondary bilayers (bottom face) recorded as a function of temperature (85 K $< T <$ 89 K) and magnetic field ($H < 90$ Oe).

0031-9007/94/72(24)/3867(4)$06.00

Assuming small current redistribution effects [13], the secondary voltage V_s is a measure of the effective coupling strength $E_c(T,H)$ of interlayer vortex correlations [14]. Since V_s is also proportional to the density of both thermally excited and magnetically induced *a-b* plane vortices $n_f^{2D}(T,H)$, as well as to the primary current I_p, we then estimate $V_s(T,H) \propto n_f^{2D}(T,H)E_c(T,H)I_p$ for small currents [15].

Figure 1 shows the magnetic field dependence of the secondary voltage V_s recorded for sample A at several temperatures spanning the interval $T_c^{ab} < T < T_c^c$. For this sample, $T_c^{ab} \approx 87.8$ K and $T_c^c \approx 88.5$ K, as determined independently by measurements (not shown) of the *a-b* plane and *c* axis current-voltage characteristics [11, 16]. Near the high end of this temperature interval, the secondary voltage V_s (at fixed primary current $I_p = 0.5$ mA) smoothly decreased from a maximum value when the external field was increased. The nonzero value of V_s at $H = 0$ in this range is attributed to the combined effect of thermally activated vortex excitations and the Josephson coupling between the top and bottom faces of the sample [11]. At lower temperatures, the H dependence of V_s displayed a pronounced peak, which gradually shifted towards higher fields and became less prominent. The inset of Fig. 1 shows the main features of this behavior for the $T \approx 87.7$ K data. As H was increased, V_s was first nearly independent of H, increased approximately linearly beyond a critical field $H_p \approx 8.0$ Oe, reached a maximum V_m at a crossover field $H_m \approx 25.0$ Oe, and finally decayed smoothly towards zero at higher fields.

In our interpretation, H_p is the field at which magnetic flux is depinned, and represents an upper limit for the penetration field [4]. Above H_p, flux is believed to enter the sample as 3D vortices in the form of strings of 2D pancake vortices, causing the secondary voltage to increase as H/Φ_0 [17] provided in-plane vortex renormalization effects are neglected. As V_s passes through its maximum value at $H = H_m$, however, the increasing in-plane vortex interaction eventually causes vortex lines to dissociate into correlated 2D vortices, with the mechanism ascribed by other workers to possible magnetic decoupling [18], entanglement [6], or evaporation [10]. Finally, at higher fields $H \gg H_m$, vortices on adjacent CuO bilayers become uncorrelated ($E_c \approx 0$) and the secondary voltage vanishes. It follows from this picture, therefore, that H_m marks a crossover from 3D vortex line behavior in the interval $H_p < H < H_m$ to 2D vortex correlation behavior for $H > H_m$. As can also be seen from Fig. 1, it is evident that both H_p and H_m vanish at $T_m \approx 88.1$ K.

Figure 2 illustrates the effect of an external magnetic field on the secondary voltage V_s for primary currents I_p (0.5–6.0 mA) for sample B. Clearly, larger primary currents depress both H_m and H_p, with the latter reaching zero at $I_p \approx 2.0$ mA. This behavior is consistent with our interpretation of H_p and H_m, since larger bias currents tend to reduce the effective pinning, interlayer vortex interaction, and increase the density of thermally excited vortices [15]. Nevertheless, we believe a reasonably accurate picture of vortex phases near the superconducting transition of Bi:2212 may be obtained when the primary bias currents are restricted to small values ($I_p \leq 0.5$ mA).

To illustrate the weak-field *H-T* phase diagram of Bi:2212, we have recorded the depinning and crossover fields (as defined in the inset of Fig. 1) for each secondary voltage curve. The resulting phase boundaries $H_p(T)$ and $H_m(T)$ are displayed in Fig. 3, along with a mean-field $H_{c2}(T) = \Phi_0/2\pi\xi^2(T)$ [8] boundary. The depinning field exhibited an unusual temperature dependence, which consisted of a pronounced drop in the vicinity of T_c^{ab} followed by a broad tail structure at higher temperatures [19]. By contrast, the 3D-2D crossover field $H_m(T)$ varied smoothly with temperature near T_c^{ab} [20], and a power-law fit yielded $H_m = H_0(T_m/T - 1)^\nu$ with $H_0 \approx 930$ Oe and $\nu \approx 0.68$.

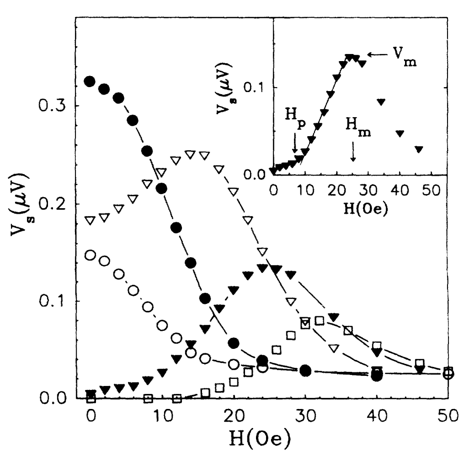

FIG. 1. H dependence of the secondary voltage V_s at 88.3 K (○), 88.1 K (●), 87.9 K (▽), 87.7 K (▼), and 87.5 K (□) for sample A and $I_p = 0.5$ mA. H_p and H_m are identified in the inset.

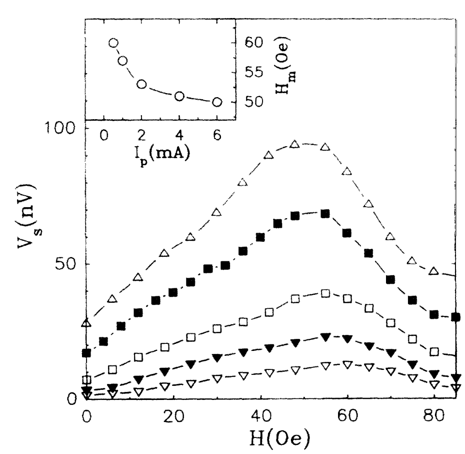

FIG. 2. H dependence of the secondary voltage V_s at $T =$ 85.3 K for sample B and $I_p = 0.5$ mA (▽), 1.0 mA (▼), 2.0 mA (□), 4.0 mA (■), and 6.0 mA (△). The inset shows H_m vs I_p.

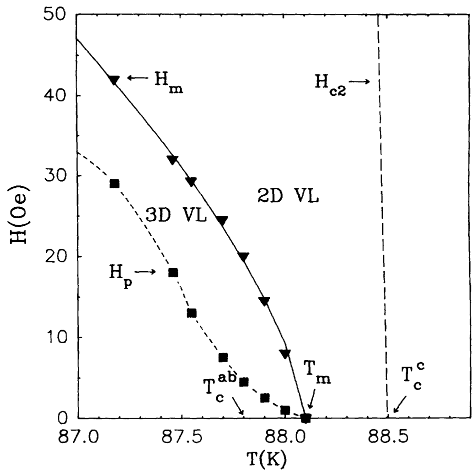

FIG. 3. *H-T* phase diagram of sample A showing the measured $H_p(T)$ (■) and $H_m(T)$ (▼) boundaries and the $H_{c2}(T)$ line [8]. H_m separates regions of 3D vortex lines and 2D vortex liquid. $T_c^{ab} \approx 87.8$ K and $T_c^c \approx 88.1$ K are measured from *IV* curves. The solid line is a power-law fit and the dotted line is a guide to the eye.

A notable feature of our findings was the appearance of a critical point T_m in the temperature interval $T_c^{ab} < T_m < T_c^c$, where the two phase lines intersected at $H_p(T_m) = H_m(T_m) = 0$. Although we observed some sample-to-sample variations, we found that T_m was consistently higher than T_c^{ab}, with $T_m - T_c^{ab} \sim 0.2 \pm 0.1$ K. This result is illustrated for sample C in Fig. 4, where the T_m and T_c^{ab} were separately determined from *a-b* plane *IV* measurements. Figure 4(a) illustrates the magnetic field dependence of the primary voltage V_p, at a fixed primary current $I_p = 10\ \mu$A, for several temperatures near T_c^{ab}. The measurements of V_p are useful, because they provide an independent way to obtain the temperature dependence of H_p. When flux penetrated freely into the sample, as for the $T = 85.7$ K curve, Fig. 4(a) shows that V_p increased linearly with field. For nonvanishing H_p, however, V_p was insensitive to the applied field until H reached H_p, above which nearly linear $V_p(H)$ curves were obtained. By identifying in this way the threshold field for each primary voltage curve, H_p was found to increase steadily with decreasing temperatures below $T_m \approx 85.7$ K, as indicated in the inset of Fig. 4(a). For comparison, Fig. 4(b) shows a set of corresponding zero-field *a-b* plane *IV* characteristics, which were taken in the same temperature interval. From the small-current *IV* exponents $a(T)$ [inset of Fig. 4(b)], we identified the *a-b* plane transition temperature $T_c^{ab} \approx 85.6$ K, and estimated $T_c^c \approx 85.9$ K [11].

The above measurements of H_p, determined from V_p, were somewhat less accurate than those determined from flux-transformer measurements; nevertheless, they yielded a critical point T_m that was ~0.1 K higher than the unbinding transition T_c^{ab} for this sample. Similar measurements in other samples also indicated a clear tendency for T_m to be ~0.2 ± 0.1 K higher than T_c^{ab}. Collectively, these results reinforce the idea that the zero-

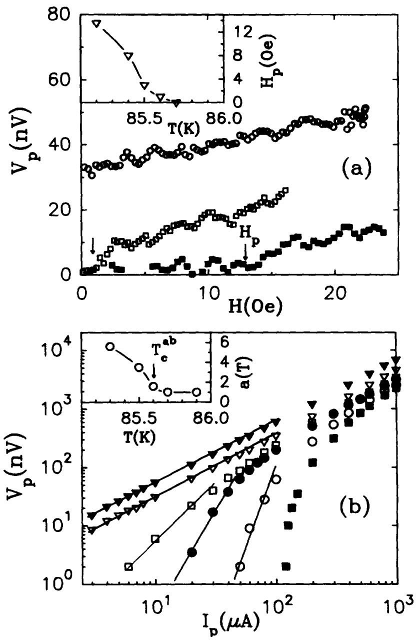

FIG. 4. (a) H dependence of the primary voltage V_p at 85.7 K (○), 85.6 K (□), and 85.2 K (■) for sample C and $I_p = 10\ \mu$A. Inset: H_p vs T. (b) Zero-field *IV* characteristics at 85.9 K (▼), 85.7 K (▽), 85.6 K (□), 85.5 K (●), 85.3 K (○), and 85.1 K (■) for sample C. Inset: *IV* exponent $a(T)$.

field resistive transition of Bi:2212 is characterized by a temperature T_m, which marks a vortex phase crossover from a region of free thermally excited 3D vortex lines ($T_c^{ab} < T < T_m$) to a region of free 2D vortices with interlayer correlations ($T_m < T < T_c^c$) [21].

An unusual feature of our vortex phase diagram (Fig. 3) is the presence of a Meissner phase boundary $H_p(T)$ which extends above T_c^{ab} to T_m [22]. Below T_c^{ab}, the observed penetration fields in Bi:2212 have recently been attributed to surface barriers of the Bean-Livingston type [2]. Another possible contribution to the Meissner phase may involve bound vortex-antivortex pairs. An isolated infinitely wide 2D superconductor, which is characterized by power-law resistivity, cannot expel flux since the lower critical field vanishes, i.e., $H_{c1} = 0$ [23]. On the other hand, a 2D film of finite width W requires a small but nonzero depairing current, approximately given by $I_W \propto 1/W$ [8], to dissociate the weakest bound vortex-antivortex pairs. As a result, no dissipation occurs for currents $I < I_W$ and the film develops a weak diamagnetic response up to a lower critical field $H_{c1} \sim (4\Phi_0/W^2)\ln(W/\xi)$ [24]. For Bi:2212, we can approximate the penetration field H_p associated with a stack of N decoupled 2D layers as $H_p \sim NH_{c1}$, where H_{c1} is the lower critical field of one isolated layer. Using $W \sim 1$ mm, $\xi(T_c^{ab}) \sim 10^2$ Å, and $N \sim 10^4$, we obtain a consistent value for $H_p \sim 10$ Oe (Fig. 3).

In the temperature interval $T_c^{ab} < T < T_m$, where the CuO bilayers are resistive, flux appears to penetrate the sample as a collection of free 3D vortex lines, which decompose [10] into interacting 2D vortices (vortex liquid) when the field exceeds H_m. In contrast to recent suggestions [4], we observe no evidence for a reentrant critical current in this region of the phase diagram. Below T_c^{ab}, where pinning effects become increasingly important [8, 23, 25], different solid phases of 3D vortex lines may form in the region $H_p < H < H_m$ of the H-T diagram. For a vortex lattice, we can use a Lindemann-like criterion to determine whether or not the lattice melts at the crossover field H_m by estimating the ratio $c_L = \Lambda/a_v$ of the thermal rms vortex displacement $\Lambda = (8\pi^2 dk_B T/\Phi_0 H_p)^{1/2}$ and the intervortex spacing $a_v = (\Phi_0/H_m)^{1/2}$ at $T = 87.2$ K for sample A [6, 8]. Using $H_p \sim 30$ Oe, $H_m \sim 42$ Oe (Fig. 3), and $d \sim 20$ μm, we find that $c_L \sim 0.25$ is within the accepted range for melting. We then conclude that our 3D-2D crossover boundary $H_m(T)$ may be interpreted as either a melting line [8] or an irreversibility line [5] below T_c^{ab}, and as an "evaporation" line above T_c^{ab}.

We thank Hu Jong Lee and Dimitrios G. Xenikos for many helpful discussions. This work was supported by D.O.E. (MISCON) through Contract No. DE-FG02-90ER45427 and by NSF Grant No. DMR 92-00122.

[1] H. Safar, E. Rodriguez, F. de le Cruz, P.L. Gammel, L.F. Schneemeyer, and D.J. Bishop, Phys. Rev. B **46**, 14 238 (1992).
[2] N. Chikumoto, M. Konczykowski, N. Motohira, and A.P. Malozemoff, Phys. Rev. Lett. **69**, 1260 (1992).
[3] H. Safar, P.L. Gammel, D.J. Bishop, D.B. Mitzi, and A. Kapitulnik, Phys. Rev. Lett. **68**, 2672 (1992).
[4] D.A. Brawner, A. Schilling, H.R. Ott, R.J. Haug, K. Ploog, and K. von Klitzing, Phys. Rev. Lett. **71**, 785 (1993).
[5] A. Schilling, R. Jin, J.D. Guo, and H.R. Ott, Phys. Rev. Lett. **71**, 1899 (1993).
[6] D.R. Nelson, Phys. Rev. Lett. **60**, 1973 (1988); D.R. Nelson and H.S. Seung, Phys. Rev. B **39**, 9153 (1989).
[7] Y. Yeshurun and A.P. Malozemoff, Phys. Rev. Lett. **60**, 2202 (1988).
[8] D.S. Fisher, M.P.A. Fisher, and D.A. Huse, Phys. Rev. B **43**, 130 (1991).
[9] P.L. Gammel, L.F. Schneemeyer, J.V. Waszczak, and D.J. Bishop, Phys. Rev. Lett. **61**, 1666 (1988); A. Houghton, R.A. Pelcovits, and S. Sudbo, Phys. Rev. B **40**, 6763 (1989); R.G. Beck, D.E. Farrell, J.P. Rice, D.M. Ginsberg, and V.G. Kogan, Phys. Rev. Lett. **68**, 1594 (1992); R. Sasik and D. Stroud, Phys. Rev. B **48**, 9938 (1993).
[10] S.N. Artemenko and A.N. Kruglov, Phys. Lett. A **143**, 485 (1990); J.R. Clem, Phys. Rev. B **43**, 7837 (1991); L.N. Bulaevskii, S.V. Meshkov, and D. Feinberg, Phys. Rev. B **43**, 3728 (1991).
[11] Y.M. Wan, S.E. Hebboul, D.C. Harris, and J.C. Garland, Phys. Rev. Lett. **71**, 157 (1993).
[12] See also Refs. [1, 11] and R. Busch, G. Ries, H. Werthner, G. Kreiselmeyer, and G. Saemann-Ischenko, Phys. Rev. Lett. **69**, 522 (1992).
[13] Y.M. Wan, S.E. Hebboul, D.C. Harris, and J.C. Garland, Physica (Amsterdam) **194-196B**, 1515 (1994).
[14] The interlayer vortex coupling energy $E_c(T, H)$ incorporates Josephson, magnetic, and, as recently proposed by J.M. Duan, Phys. Rev. Lett. **70**, 3991 (1993), Coulomb interactions.
[15] For large primary currents, both n_f^{2D} and E_c may be nonlinear functions of I_p.
[16] L.N. Bulaevskii, M. Ledvij, and V.G. Kogan, Phys. Rev. Lett. **68**, 3773 (1992), also define two transition temperatures T_s and T_{c0}, which correspond to the spontaneous creation of vortex lines and the mean-field transition, respectively.
[17] Note that for $T > T_c^{ab}$, thermally excited vortices contribute to V_s even when $H = 0$, as discussed in Ref. [11].
[18] J.W. Ekin, B. Serin, and J.R. Clem, Phys. Rev. B **9**, 912 (1974); J.R. Clem, Phys. Rev. B **12**, 1742 (1975); J.W. Ekin and J.R. Clem, Phys. Rev. B **12**, 1753 (1975).
[19] A similar behavior was noted for $Tl_2Ba_2CaCu_2O_x$ crystals by V.N. Kopylov, T.G. Togonidze, and I.F. Schegolev, Physica (Amsterdam) **195C**, 379 (1992), who extracted $H_p(T)$ from magnetization measurements.
[20] H.J. Jensen and P. Minnhagen, Phys. Rev. Lett. **66**, 1630 (1991), have shown that external fields suppress the unbinding transition, with $T_c^{ab}(H)/T_c^{ab}(H = 0) = 1 - H/H_{c2}(T = 0)$. Since $H \ll H_{c2}(0)$, this effect can be neglected in our experiments.
[21] Our crossover T_m may correspond to the 3D transition recently discussed by B. Horovitz, Phys. Rev. B **47**, 5947 (1993).
[22] The origin of weak diamagnetism in the interval $T_c^{ab} < T < T_m$, where CuO bilayers are resistive, is not understood. We speculate that the interlayer Josephson interaction in a thermally excited 3D vortex line leads to an effective edge barrier potential.
[23] D.S. Fisher, Phys. Rev. B **22**, 1190 (1980).
[24] S. Doniach and B.A. Huberman, Phys. Rev. Lett. **42**, 1169 (1979).
[25] See also J.C. Garland and Hu Jong Lee, Phys. Rev. B **36**, 3638 (1987).